Metabolomics (2015) 11:380–390
DOI 10.1007/s11306-014-0699-x

ORIGINAL ARTICLE

Anti-malarial drug artesunate restores metabolic changes in experimental allergic asthma

Wanxing Eugene Ho · Yong-Jiang Xu · Fengguo Xu · Chang Cheng · Hong Yong Peh · Shao-Min Huang · Steven R. Tannenbaum · Choon Nam Ong · W. S. Fred Wong

Received: 5 April 2014 / Accepted: 30 June 2014 / Published online: 16 July 2014

Abstract The anti-malarial drug artesunate possesses anti-inflammatory and anti-oxidative actions in experimental asthma, comparable to corticosteroid. We hypothesized that artesunate may modulate disease-relevant metabolic alterations in allergic asthma. To explore metabolic profile changes induced by artesunate in allergic airway inflammation, we analysed bronchoalveolar lavage fluid (BALF) and serum from naïve and ovalbumin-induced asthma mice treated with artesunate, using both gas and liquid chromatography-mass spectrometry metabolomics. Pharmacokinetics analyses of serum and lung tissues revealed that artesunate is rapidly converted into the active metabolite dihydroartemisinin. Artesunate effectively suppressed BALF total and differential counts, and repressed BALF Th2 cytokines, IL-17, IL-12(p40), MCP-1 and G-CSF levels. Artesunate had no effects on both BALF and serum metabolome in naïve mice. Artesunate promoted restoration of BALF sterols (cholesterol, cholic acid and cortol), phosphatidylcholines and carbohydrates (arabinose, mannose and galactose) and of serum 18-oxocortisol, galactose, glucose and glucouronic acid in asthma. Artesunate prevented OVA-induced increases in pro-inflammatory metabolites from arginine–proline metabolic pathway, particularly BALF levels of urea and alanine and serum levels of urea, proline, valine and homoserine. Multiple statistical correlation analyses revealed association between altered BALF and serum metabolites and inflammatory cytokines. Dexamethasone failed to reduce

Wanxing Eugene Ho and Yong-Jiang Xu have contributed equally to this work.

Electronic supplementary material The online version of this article (doi:10.1007/s11306-014-0699-x) contains supplementary material, which is available to authorized users.

W. E. Ho · Y.-J. Xu · F. Xu · S.-M. Huang · C. N. Ong (✉)
Saw Swee Hock School of Public Health, National University Health System, National University of Singapore, 16 Medical Drive MD3, Singapore 117597, Singapore
e-mail: ephocn@nus.edu.sg

W. E. Ho · S. R. Tannenbaum
Singapore-MIT Alliance for Research and Technology (SMART), 1 CREATE Way, #03-12/13/14 Enterprise Wing, Singapore 138602, Singapore

Y.-J. Xu
Key Laboratory of Insect Development and Evolutionary Biology, Chinese Academy of Sciences, Shanghai 200023, China

F. Xu
Key Laboratory of Drug Quality Control and Pharmacovigilance, China Pharmaceutical University, Nanjing 210009, China

C. Cheng · H. Y. Peh · W. S. F. Wong
Department of Pharmacology, Yong Loo Lin School of Medicine, National University Health System, 28 Medical Drive, #03-05, Center for Life Sciences, Singapore 117456, Singapore

S. R. Tannenbaum
Department of Biological Engineering and Chemistry, Massachusetts Institute of Technology, ROOM 56-731A, Cambridge, MA 02139-4307, USA

C. N. Ong
NUS Environmental Research Institute, National University of Singapore, #02-01, T-Lab Building, 5A Engineering Drive 1, Singapore 117411, Singapore

W. S. F. Wong (✉)
Immunology Program, Life Science Institute, National University of Singapore, 28 Medical Drive, #03-05, Center for Life Sciences, Singapore 117456, Singapore
e-mail: phcwongf@nus.edu.sg

urea level and caused widespread changes in metabolites irrelevant to asthma development. Here we report the first metabolome profile of artesunate treatment in experimental asthma. Artesunate restored specific metabolic perturbations in airway inflammation, which correlated well with its anti-inflammatory actions. Our metabolomics findings further strengthen the therapeutic value of using artesunate to treat allergic asthma.

Keywords Metabolome · Artemisinins · Mass spectrometry · Allergic asthma · Corticosteroid

1 Introduction

Artesunate is a semi-synthetic analogue of the anti-malarial agents known as artemisinins. By the addition of a hemisuccinate group, artesunate is more water-soluble with greater bioavailability and better pharmacological profile (Newton et al. 2000). Apart from its effective anti-malarial actions, artesunate has promising anti-inflammatory potential in animal models of rheumatoid arthritis (Mirshafiey et al. 2006; Li et al. 2013), systemic lupus erythematosus (Jin et al. 2009) and bacteria-induced sepsis (Li et al. 2010; Jiang et al. 2011). Recently, studies have demonstrated broad anti-inflammatory and anti-oxidative properties of artesunate in experimental allergic asthma (Cheng et al. 2011; Ho et al. 2012). In addition, artesunate could prevent IgE-mediated mast cell degranulation in experimental anaphylaxis models (Cheng et al. 2013). A comprehensive report of the broad pharmacological effects of artemisinins and artesunate has been summarized in our recent review (Ho et al. 2014a).

Metabolomics refers to the global investigation of metabolites in biological systems (comparing normal to disease) (Xu et al. 2014), and has been applied to allergic asthma to profile metabolic changes and identify disease biomarkers (Lara et al. 2008; Ho et al. 2013, 2014b; Saude et al. 2009, 2011; Mattarucchi et al. 2012; Jung et al. 2013). We have recently uncovered novel disease-relevant metabolic changes in the bronchoalveolar lavage fluid (BALF) from experimental mouse asthma, which involved major losses of sugars with resultant increases in energy metabolites and reductions of sterols (Ho et al. 2013, 2014b). In the earlier study, dexamethasone reversed most metabolic alterations in allergic airway inflammation, but also induced considerable changes in other metabolites irrelevant to asthma pathogenesis. In the present study, we investigated if artesunate can afford similar protective metabolic changes in experimental allergic asthma.

Our kinetic study in mice revealed rapid conversion of artesunate to the active metabolite dihydroartemisinin (DHA), and that DHA was detectable in lung tissues. We reported the first metabolome profile of experimental asthma treated with artesunate. Artesunate restored specific metabolic perturbations in airway inflammation, which correlated well with its anti-inflammatory actions. Metabolomics data provide further evidence to support the therapeutic value of artesunate for asthma.

2 Materials and methods

Additional methods are available in the online supplement.

2.1 Animals

Female BALB/c mice, 6–8 weeks old (Canning Vale, Western Australia, Australia), were sensitized and challenged with ovalbumin (OO) to develop experimental asthma as described (Cheng et al. 2011; Ho et al. 2012). Artesunate (30 mg/kg) was dissolved in 5 % DMSO, given intraperitoneally (i.p.) to naïve (N/Arts) and OVA-challenged mice (OO/Arts) an hour prior to each aerosol challenge. Vehicle controls (OO/DMSO) received the same regime of 5 % DMSO (i.p.). Animal experiments were performed according to the Institutional guidelines for Animal Care and Use Committee of the National University of Singapore.

2.2 BALF and serum collection and analysis

Mice were anesthetized 24 h after the last aerosol challenge and cardiac puncture and BAL were performed (Cheng et al. 2011). Blood was collected 5 min post-anaesthesia and incubated at room temperature for 1 h prior centrifugation for serum collection. Total and differential cell counts were determined from BALF collected as described previously (Cheng et al. 2011). BALF and serum supernatants were frozen at −80 °C prior further analysis. Cell count data and BALF metabolomic data of experimental asthma (OO), saline controls (OS) and naïve mice (N) were presented in an earlier study with the publisher's consent for usage of raw data for further analysis (Ho et al. 2013).

2.3 Artesunate pharmacokinetics

Artesunate (30 mg/kg) was given i.p. to naïve mice (n = 6 per time point) and anesthetized prior to collection of blood and lung tissues at various time points. Serum (50 µl) or lyophilized lung tissue (2 mg) was mixed with 200 µl of methanol containing 5 µg/ml of FMOC-glycine (Sigma-Aldrich, St. Louis, MO, USA) as internal standard. LC/MS was employed to measure concentrations of artesunate and DHA in serum and lung tissues. LC/MS analysis was

performed using an Agilent 1100 HPLC system (Santa Clara, CA, USA) connected to LCQ FLEET Ion-Trap Mass detector with Atmospheric Pressure Chemical Ionization (APCI+) (Thermo Scientific, Waltham, MA, USA). The column used was Inertsil ODS-3 (3 μm, 3.0 × 150 mm) at room temperature, with a mobile phase of HPLC grade methanol and 0.1 % formic acid (80:20) at a flow rate of 0.4 ml/min. Artesunate and DHA concentrations were calculated based on seven-point dilution range of spiked artesunate and DHA pure standards (10–1,000 ng/ml) in pooled naïve mice sera or lung tissues.

2.4 BALF cytokine analysis

Cytokines were assayed using a murine Luminex bead-based suspension array system (Bio-Rad, CA, USA) and analysed using a Bio-Plex Array Reader (Bio-Rad) according to manufacturer's instructions.

2.5 Metabolomics sample pretreatment

Aliquots of BALF (400 μl) were concentrated using a freeze-dryer (Labconco Corporation, Kansas City, USA) at −85 °C and reconstituted using 200 μl ice-cold methanol spiked with 10 μg/ml FMOC-glycine as internal standard. The solution was vortexed (3 min) and ultrasonically extracted (15 min, 4 °C). After two centrifugations (16,000 rcf × 10 min, 4 °C), the supernatant were divided into two portions: 70 μl for LC–MS analysis directly and the other 70 μl for GC–MS analysis.

2.6 GC/MS analysis

GC/MS derivatization was based on the method previously described (Xu et al. 2009). Briefly, 1.0 μl derivatized supernatant was injected splitlessly with an Agilent 7683 Series autosampler into an Agilent 6890 GC system equipped with a HP-5MSI column. The inlet temperature was set at 250 °C. Helium was used as the carrier gas at a constant flow rate of 1.0 ml/min. The column temperature was initially maintained at 70 °C for 1 min, and then increased to 250 °C at a rate of 10 °C/min and further increased at 25 °C/min to 300 °C where it remained for 5 min. The column effluent was introduced into the ion source of an Agilent Mass selective detector. The transfer line temperature was set at 280 °C and the ion source temperature at 230 °C. The mass spectrometer was operated in electron impact mode (70 eV). Data acquisition was performed in full scan mode from *m/z* 50-550 with a scan time of 0.5 s. Compounds were identified by comparison of mass spectra and retention time with those of reference standards, and those available in libraries (NIST 5).

2.7 LC/MS analysis

LC–MS analysis was performed on an Agilent 1200 HPLC system equipped with 6410 QQQ mass detector. Pre-treated BALF supernatant (5 μl) was injected into the HPLC system and managed by a MassHunter workstation. The column used for the separation was an Agilent rapid resolution HT zorbax SB-C18 (2.1 × 50 mm, 1.8 μm) (Agilent Technologies, Santa Clara, CA). The oven temperature was set at 50 °C. The gradient elution involved a mobile phase consisting of (A) 0.1 % formic acid in water and (B) 0.1 % formic acid in methanol. The initial condition was set at 5 % of B. The following solvent gradient was applied: from 95 % A and 5 % B to 10 % A and 90 % B within 10 min, hold for 10 min and then to 100 % B within 5 min and hold for 10 min. Flow rate was set at 0.2 ml/min and 5 μl of samples were injected. The ESI-MS were acquired in positive and negative ion mode, respectively. The ion spray voltage was set at 3,000 V. The heated capillary temperature was maintained at 350 °C. The drying gas and nebulizer nitrogen gas flow rates were 10 l/min and psi, respectively. For full scan mode analysis spectra were stored from *m/z* 100 to 1,000. Compounds showing significant differences between groups were searched in the Human Metabolome Database (HMDB, www.hmdb.ca) using mass-to-charge ratio (*m/z*) and identified by either MS/MS fragmentation patterns from HMDB, METLIN or reference standards.

2.8 Data pre-processing

Each chromatogram obtained from GC/MS and LC/MS analysis was processed for baseline correction and area calculation using MZmine 2.0 software package (Pluskal et al. 2010). Data were combined into a single matrix by aligning peaks with the same mass and retention time for GC/MS and LC/MS data, respectively. Area of each peak was normalized to that of internal standard FMOC-glycine in each data set. The missing values were replaced with a half of the minimum value found in the data set (Ng et al. 2012). Ninety percent filtering was applied to the raw data to include only metabolites that were detectable in 90 % of the subjects in at least one of the treatment groups to ensure selection of relevant metabolites.

2.9 Statistical analysis

One-way ANOVA followed by Dunnett's test was used to determine significant differences in cell counts and cytokines between groups, with significant levels at $p < 0.05$. Correlations between metabolites and inflammatory cells were calculated using Pearson's correlation analysis. Multivariate statistical analysis was performed using

SIMCA-P software version 11.0 (Umetrics AB, Umea, Sweden). Orthogonal projections to latent structures discriminant analysis (OPLS-DA) was used to model the discrimination between control and treatment groups by visualization of score plots. Prior to OPLS-DA, data were mean-centered and unit variance scaled. Metabolites heatmap and nonparametric test (Wilcoxon, Mann–Whitney test) were conducted using MultiExperiment View V4.6.1 (www.tm4.org).

3 Results

3.1 Artesunate is rapidly converted to DHA

Upon administration of 30 mg/kg artesunate, we observed a rapid conversion of artesunate to its active metabolite DHA within 5 min. Maximum serum artesunate concentration was achieved at 5 min, while maximum serum DHA concentration was observed at 15 min (Fig. 1a). Artesunate was completely metabolized within 1 h, while serum DHA level persisted for 6 h. Lung DHA concentration peaked at 10 min and achieved steady states from 15 min to 6 h (Fig. 1b). Lung artesunate level was not detectable.

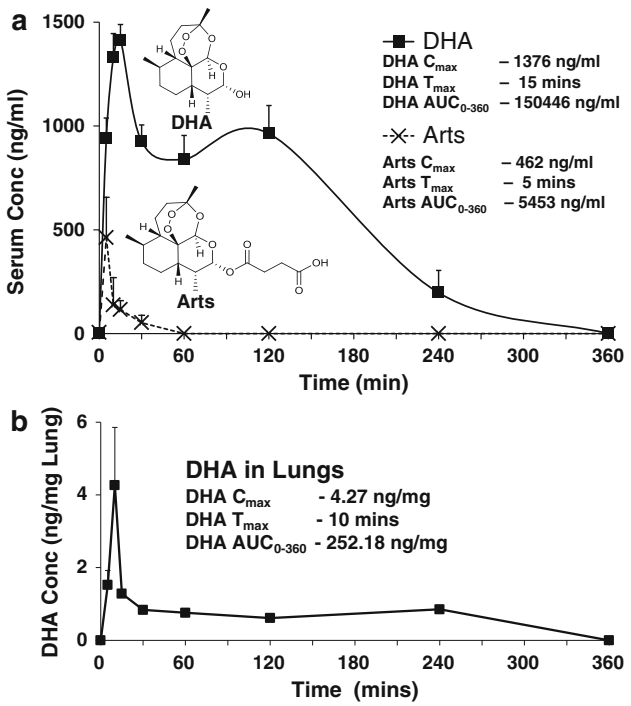

Fig. 1 Kinetic profiling of artesunate and active metabolite DHA. Pharmacokinetic analyses of serum and lungs tissues were performed after a single intra-peritoneal dose of artesunate (30 mg/kg) was given to naïve mice. **a** Serum levels of artesunate (Arts) and DHA were measured using liquid-chromatography–mass spectrometry (LC/MS), at various time points post administration. **b** Concentrations of DHA in lung tissues (ng/ml) collected at various time points post administration. Each data point represents the mean drug concentration ± SEM in serum or lung tissues (n = 6 mice per time point)

3.2 Artesunate does not alter metabolite profiles in naïve mice

In OPLS-DA analysis, the value of R^2Y describes how well the data in the training set are mathematically reproduced, ranging between 0 and 1, where 1 indicates a model with a perfect fit. Models with a Q^2 value greater than or equal to 0.5 are generally considered to have good predictive capability. Our analysis by GC/MS (Fig. S1a, c) and LC/MS (Fig. S1b, d) revealed poor R^2Y and Q^2 values, indicating no distinctive changes in both BALF and serum metabolic profiles between untreated naïve mice (N) and artesunate-treated naïve mice (N/Arts). In line with these findings, artesunate did not alter BALF inflammatory cell counts in naïve mice (Fig. 2a), and showed no toxic effects on human bronchial epithelial cells or mouse peripheral blood cells (Fig. S3).

3.3 Drug vehicle does not affect metabolic profiles in experimental asthma

OPLS-DA analysis revealed little difference in BALF metabolite profiles between OVA-sensitized and -challenged mice (OO) and OO treated with vehicle control DMSO (OO/DMSO), as indicated by poor modeling scores R^2Y (0.56 and 0.79) and predictive Q^2 values (0.0126 and 0.00477) detected by GC/MS (Fig. S2a) and LC/MS (Fig. S2Sb), respectively. The R^2Y (0.424 and 0.638) values (Fig. S2c) and predictive Q^2 scores (−0.111 and −0.126) (Fig. S2d) demonstrated equally poor separations between OO and OO/DMSO for serum metabolic profiles. DMSO did not affect BALF inflammatory cell counts in both naïve and OO mice (Fig. 2a) or cause cytotoxicity to human bronchial epithelial cells (Fig. 3S).

3.4 Artesunate suppresses airway inflammation and restores metabolic changes in experimental asthma

We re-analysed published cell counts and BALF metabolomics data of naïve mice (N), saline-controls (OS) and experimental asthma (OO) with publisher's consent (Ho et al. 2013), together with new artesunate-treatment groups. Artesunate (30 mg/kg) effectively suppressed pulmonary eosinophilia with moderate inhibition on lymphocyte and neutrophil counts (Fig. 2a). Besides, artesunate subdued OVA-induced elevation of IL-4, IL-5, IL-13, IL-17, IL-12 p(40), MCP-1 and G-CSF (Fig. 2b–f). Artesunate was able to alter BALF metabolite profiles as detected by GC/MS

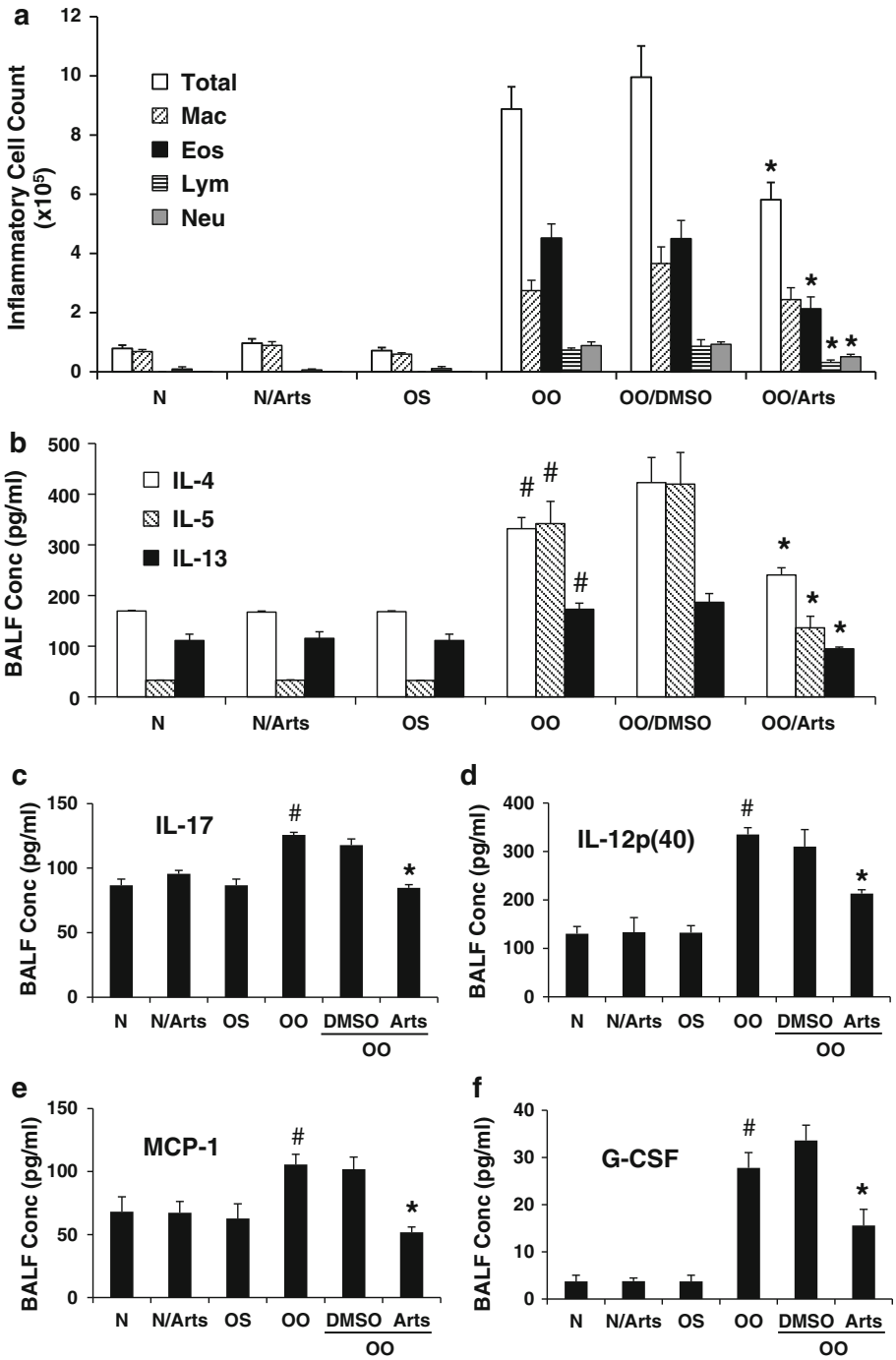

Fig. 2 Artesunate suppresses airway inflammation and inflammatory cytokine levels in experimental asthma. **a** Inflammatory cell numbers in the BALF were enumerated by total and differential cell counts. *Total* total inflammatory cells, *Mac* macrophages, *Eos* eosinophils, *Lym* lymphocytes and *Neu* neutrophils. Cell numbers are expressed as mean ± SEM (n = 8–12 per treatment group). #Statistical significance as compared to OS, $p < 0.05$, while *statistical significance as compare to OO/DMSO, $p < 0.05$. **b** BALF levels of Th2 cytokines, IL-4, IL-5 and IL-13, **c** IL-17, **d** IL-12 (p40), **e** MCP-1 (E) and **f** G-CSF. Cytokine levels are expressed as mean ± SEM (n = 6 per treatment group). #Statistical significance as compared to OS, $p < 0.05$, while *statistical significance as compare to OO/DMSO, $p < 0.05$

(Fig. 3a) and LC/MS (Fig. 3b), with strong R^2Y (0.993 and 0.893) and Q^2 (0.747 and 0.738) values, indicating distinctive separation of BALF metabolites among N, OO and OO/Arts mice. Statistical analysis revealed a total of 19 BALF metabolites were significantly altered by artesunate (Fig. 3c, d), and it could restore OVA-induced changes in 12 metabolites (Fig. 3c, S4). Artesunate reversed the fall in carbohydrates galactose, mannose and arabinose in experimental asthma. Drops in sterols and related bile acid cholesterol, cortol and cholic acid were also increased by artesunate. Similarly, artesunate replenished losses in 5 phosphatidycholines (PC) including PC 32:0, PC 34:1, PC 34:2, PC 34:3, PC 35:5. In contrast, the increases in energy metabolites and amino acids such as lactate, choline, urea, alanine and acetamide in experimental asthma were suppressed by artesunate. On the other hand, six BALF

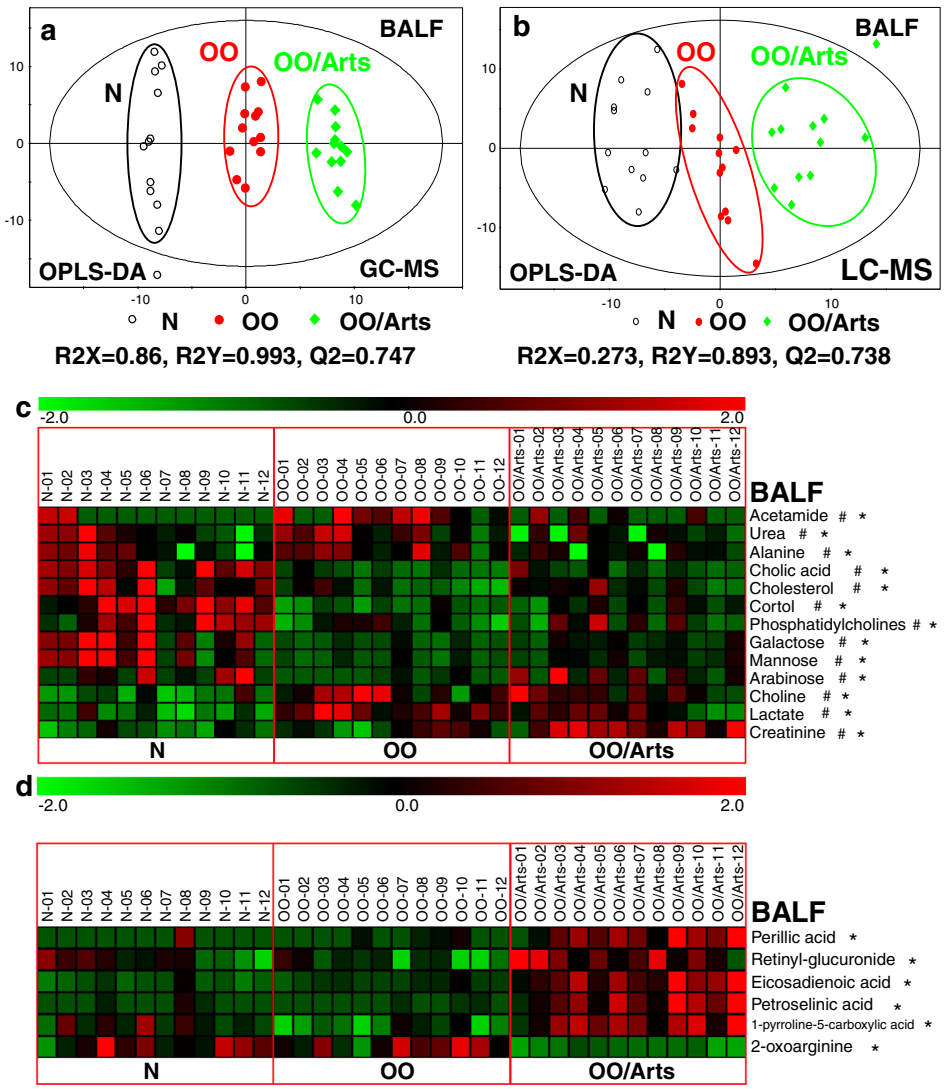

Fig. 3 Artesunate reverses lung global metabolic profile altered in experimental asthma. OPLS-DA of lung metabolites in the BALF of naïve mice (N), OVA-sensitized and -challenged mice (OO), and OO-treated with artesunate (OO/Arts) detected by **a** GC–MS analysis or **b** LC–MS analysis. R^2Y describes the goodness of mathematical modelling of the data; while Q^2 values of 0.5 or more are considered to have good predictive capability. *Black open circles*, N (n = 12); *red filled circles*, OO (n = 12); *green filled diamonds*, OO/Arts (n = 12). The x axis, t[1], and y axis, t[2], indicate the first and second principle components, respectively. **c** Significant fold changes in BALF metabolites are expressed as a heatmap for N, OO and OO/Arts, detected by either LC/MS or GC/MS. #Significant changes in OO versus N, $p < 0.05$. *Significant changes in OO/Arts versus OO, $p < 0.05$. **d** Additional BALF metabolites irrelevant to asthma changed by artesunate are expressed as a heatmap for N, OO and OO/Arts, detected by either LC/MS or GC/MS. Fold changes are derived from the fold difference over normalized, mean-centered values for each metabolite. *Green square* indicates a reduction of up to twofolds, *black square* indicates no significant fold change, and *red square* indicates an increase of up to twofolds. *Significant changes in OO/Arts versus OO, $p < 0.05$ (Color figure online)

metabolites irrelevant to experimental asthma were altered by artesunate (Fig. 3d, S4). Pearson correlation analysis revealed moderate to strong correlations of 10 BALF metabolites to various inflammatory cytokines as shown in Table S1. In particular, IL-4, IL-5, IL-17, IL-12 p(40) and G-CSF were significantly ($p < 0.05$) correlated with urea, choline, lactate, carbohydrates (arabinose, galactose and mannose), sterols (cholesterol, cholic acid and cortol), and phosphatidylcholines.

3.5 Artesunate reverses metabolic changes in serum in experimental asthma

From GC/MS and LC/MS analyses (Fig. 4a, b), experimental asthma (OO) serum profile shifted from OS and N could be clearly observed with strong R^2Y (0.811 and 0.962) as well as Q^2 (0.708 and 0.632) values. When treated with artesunate (OO/Arts) or dexamethasone (OO/Dex), serum metabolic profiles distinctive from

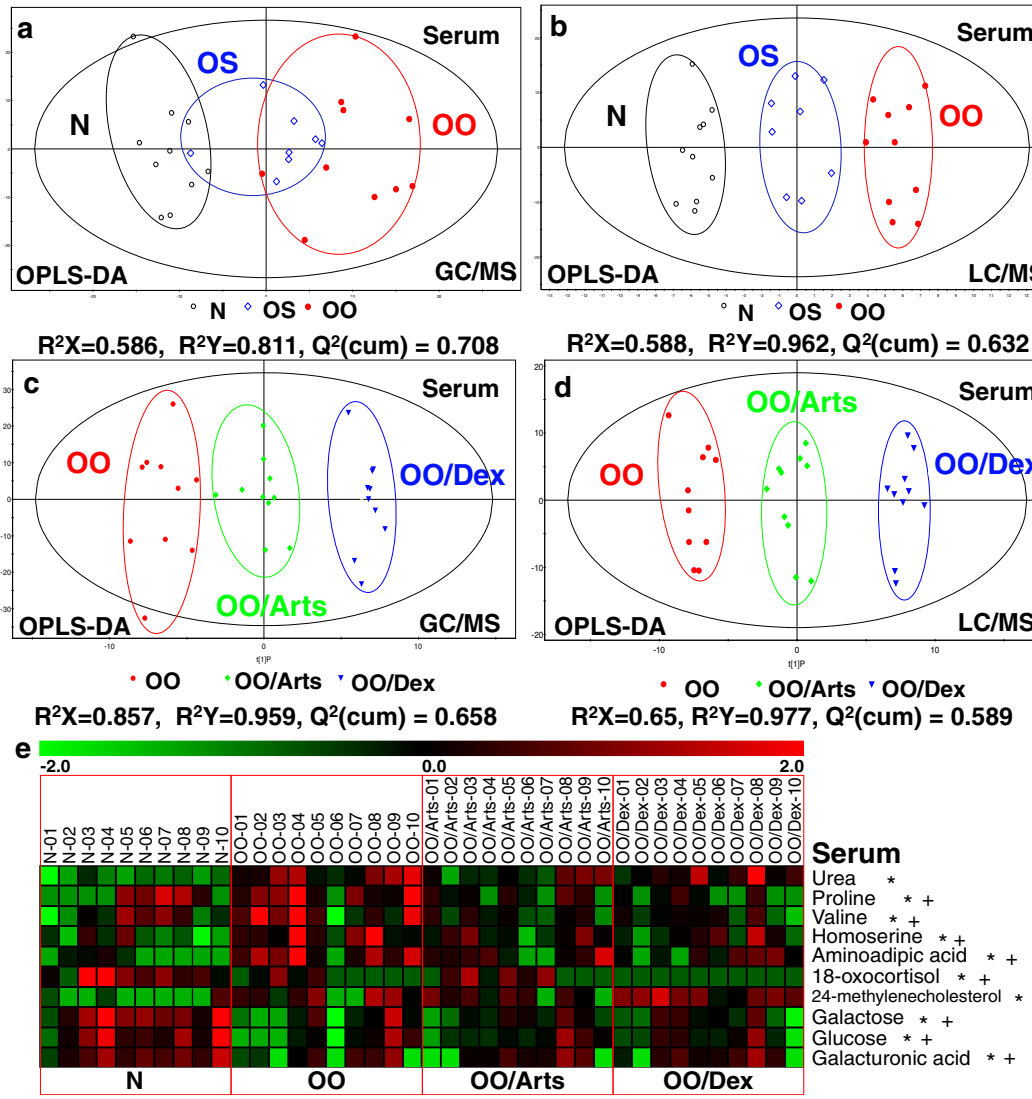

Fig. 4 Global serum metabolomics profiling in experimental asthma treated with artesunate and dexamethasone. OPLS-DA of global serum metabolite changes in N, OS OO OO/Arts and OO/Dex mice detected by GC/MS (**a**, **c**) or LC/MS (**b**, **d**) are shown. R^2Y describes the goodness of mathematical modelling of the data; while Q^2 values of 0.5 or more are considered to have good predictive capability. *Black open circles*, N (n = 10); *blue open circles*, OS (n = 10); *red filled circles*, OO (n = 10); *green filled diamonds*, OO/Arts (n = 10); *blue triangles*, OO/Dex (n = 10). The x axis, t[1], and y axis, t[2], indicate the first and second principle components, respectively. **e** Significant fold changes in serum metabolites are expressed as a heatmap for N, OO, OO/Arts and OO/Dex, detected by either LC/MS or GC/MS. Fold changes are derived from the fold difference over normalized, mean-centered values for each metabolite. *Green square* indicates a reduction of up to twofolds, *black square* indicates no significant fold change, and red square indicates an increase of up to twofolds. *Significant changes in OO/Arts versus OO, $p < 0.05$. $^+$Significant changes in OO/Dex versus OO, $p < 0.05$ (Color figure online)

experimental asthma (OO) could be observed with robust R^2Y (0.959 and 0.977) and Q^2 (0.658 and 0.589) values (Fig. 4c, d). An overview of 10 serum metabolite changes induced by artesunate and dexamethasone are represented in a heatmap (Fig. 4e). Artesunate suppressed the increase in serum urea, proline, valine, homoserine and aminoadipic acid in experimental asthma (Fig. 4e, S5). In contrast, artesunate reversed the fall in serum carbohydrates galactose, glucose and galacturonic acid in asthma. As for serum sterols, artesunate reversed the drop in 18-oxocortisol and halted the elevation of 24-methylenecholesterol in asthma. Dexamethasone demonstrated some differential metabolic effects, for instance, failing to reverse the drop in 18-oxocortisol or to block the increase in urea and 24-methylenecholesterol in experimental asthma.

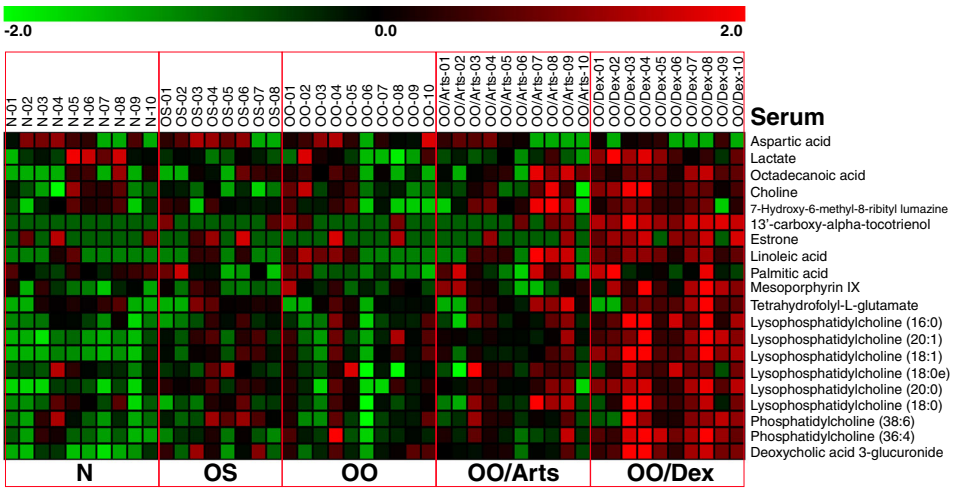

Fig. 5 Artesunate does not induce additional significant metabolic effects in the serum. Additional serum metabolites irrelevant to asthma changed by dexamethasone are expressed as a heatmap for N, OS, OO, OO/Arts and OO/Dex, detected by either LC/MS or GC/MS. Fold changes are derived from the fold difference over normalized, mean-centered values for each metabolite. *Green square* indicates a reduction of up to twofolds, *black square* indicates no significant fold change, and *red square* indicates an increase of up to twofolds (Color figure online)

3.6 Correlation of metabolite changes between serum and BALF in experimental asthma

Pearson correlation analysis revealed that alterations in serum urea, homoserine, aminoadipic acid and 18-oxo-cortisol were strongly associated with changes in BALF urea, cholic acid, cholesterol, cortol, lactate and sugars such as arabinose, galactose and mannose (Table S2). These findings provide a primary indication that systemic serum metabolome may be linked to corresponding pulmonary metabolic changes in allergic asthma.

3.7 Dexamethasone causes additional changes in serum metabolites irrelevant to experimental asthma

An assembly of twenty serum metabolites were found to be significantly modulated by dexamethasone (19 up-regulated and 1 down-regulated), which were unaltered in N, OS, OO and OO/Arts groups (Fig. 5). Artesunate did not cause any additional serum metabolic changes similar to those by dexamethasone, indicating that these two anti-inflammatory agents confer dissimilar metabolic effects in experimental asthma.

4 Discussion

Mechanistically, we have demonstrated that artesunate possesses anti-inflammatory and anti-oxidative effects on multiple cell types, such as epithelial cells, airway smooth muscle cells and various inflammatory cells in experimental asthma, via modulation of transcription factors, Nrf2 and PI3K/Akt (Cheng et al. 2011; Ho et al. 2012; Tan et al. 2013). Notably, our earlier study has demonstrated that artesunate was capable of suppressing the development of airway hyperresponsiveness in the allergic asthma model (Cheng et al. 2011). Recently, our laboratory has reported the first metabolomics study on BALF from mouse asthma, and revealed major changes in carbohydrates, sterols and energy metabolites (Ho et al. 2013). Our subsequent followup metabolomics study of house dust mite-induced allergic asthma similarly demonstrated corroborating and comprehensive evidences of altered pulmonary metabolism in the lung tissues, BALF and serum (Ho et al. 2014b). The present study investigated the metabolomics of serum from asthma mice, and evaluated potential restorative effects of artesunate in BALF and serum metabolome of allergic asthma in comparison with dexamethasone. We presented the first kinetic study of artesunate in mice showing rapid conversion to DHA, the major active metabolite (Teja-Isavadharm et al. 2001; Morris et al. 2011), within 1 h after i.p. administration. DHA was detectable in lung tissues, indicating this active metabolite is likely mediating the protective effects of artesunate in experimental asthma (Cheng et al. 2011; Ho et al. 2012).

In addition to the inhibition of OVA-induced pulmonary infiltration of eosinophils, lymphocytes and neutrophils, and increase in Th2 cytokine IL-4, IL-5 and IL-13 in the allergic airway (Ho et al. 2012; Cheng et al. 2011), artesunate was able to reduce the BALF level of a broad range of pro-inflammatory cytokines including IL-17, MCP-1, IL-12 p(40) and G-CSF. IL-12 p(40) has been linked to the full-blown asthma phenotype (Meyts et al. 2006) and G-CSF is a major survival factor for neutrophils (Dai et al. 2012).

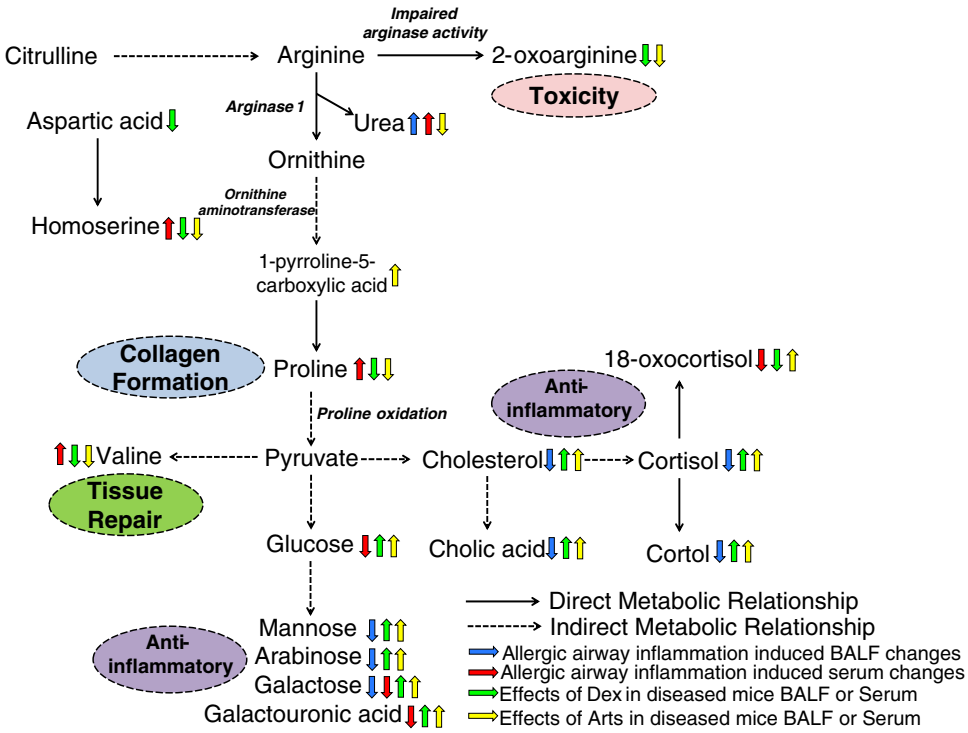

Fig. 6 Overview of disease-associated metabolites involved in allergic airway inflammation and altered by artesunate or dexamethasone. Metabolites relationships are derived from Human Metabolome Database (HMDB) and existing literatures

We have reported that BALF levels of sterols such as cholesterol, cholic acid and cortol declined in asthma model (Ho et al. 2013). Serum level of 18-oxocortisol, a cortisol metabolite, was also found reduced in experimental asthma. Serum cholesterol level is inversely related to asthma and wheeze (Fessler et al. 2009). Cholesterol and cortol are respective upstream and downstream metabolites of cortisol, an endogenous anti-inflammatory sterol (Peebles et al. 2000). Artesunate was able to restore the BALF levels of cholesterol, cholic acid and cortol, and serum level of 18-oxocortisol, which were correlated to the reductions of IL-4, 5, 13, 17 and 12(p40), MCP-1 and G-CSF levels, and may be linked to its anti-inflammatory effects in asthma.

There appears to be a causal link between PC and lung surfactants levels, where reduction in PC level can lead to worsening in lung functions in asthma (Wright et al. 2000; Ried et al. 2013). BALF level of PC dipped, but its downstream metabolite choline level elevated in experimental asthma (Ho et al. 2013). Choline, when given in excess as supplement, has also been found to exert anti-oxidative and anti-inflammatory effects in asthma (Mehta et al. 2009, 2010). Artesunate promoted recoveries of five PCs, PC 32:0, PC 34:1, PC 34:2, PC 34:3, PC 35:5, and prevented the adaptive increase in choline level in the allergic airways. These data are strongly correlated with the drops in BALF pro-inflammatory cytokines, and may contribute to the suppression airway hyperresponsiveness and restoration of lung dynamic compliance as previously reported (Cheng et al. 2011). Aminoadipic acid is a metabolic marker for protein carbonyl oxidation, linking to tissue proteolysis and oxidative stress in sepsis, diabetes and renal failure (Sell et al. 2007). In this study, OVA-induced increase in serum aminoadipic acid was suppressed by both artesunate and dexamethasone, probably as a result of lessening oxidative stress in asthma (Ho et al. 2012).

In asthma, BALF lactate is the energy metabolite being most prominently elevated, and is strongly correlated to increased pro-inflammatory cytokine levels, suggesting enhanced energy burden in allergic airway inflammation. Artesunate significantly lowered the level of lactate in BALF. In contrast, dexamethasone failed to halt lactate increase in BALF (Ho et al. 2013), but further raised lactate serum level in asthma.

Both artesunate and dexamethasone suppressed the rise in glucogenic amino acids (e.g. proline, valine, homoserine and alanine), but reversed the drop in glucose, mannose, galactose, arabinose and galacturonic acid in asthma. The arginine-proline pathway is implicated in asthma (Meurs et al. 2002; Lara et al. 2008), whereby increase in arginase activity can lead to augmented conversion of L-arginine to urea and ornithine. Ornithine is converted to proline and then to valine (Weeda et al. 1980). Proline is associated with increased collagen formation (Barbul 2008; Lara et al. 2008), while valine is linked to tissue repair (Smith and Sun 1995). These findings suggest that artesunate and dexamethasone could limit arginine-proline metabolism in asthma (Fig. 6). Nevertheless, dexamethasone failed to suppress serum urea significantly.

Glucogenic amino acids can be metabolized into glucose via gluconeogenesis, suggesting that both artesunate and dexamethasone may promote glucose, mannose, galactose and arabinose levels via gluconeogenesis in experimental asthma (Fig. 6). Galactose and mannose shared strong negative correlations with inflammatory cell counts (Ho et al. 2013) and with inflammatory cytokines observed in the present study. Mannose possesses broad anti-inflammatory effects against LPS-induced lung injury (Xu et al. 2008), while the product of arabinose and galactose, arabinogalactan, exhibits protection against allergic asthma (Peters et al. 2010).

Dexamethasone caused changes in 20 BALF metabolites which were unaltered in experimental asthma (Ho et al. 2013). In contrast, artesunate only induced changes in 6 BALF metabolites that were irrelevant to asthma development. Petroselinic acid was induced but 2-oxoarginine was reduced by both artesunate and dexamethasone. Elevation in petroselinic acid can suppress arachidonic acid which is a key lipid mediator that promotes airway inflammation (Weber et al. 1995; Serrano-Mollar and Closa 2005). Reduction of 2-oxoarginine may help lessen certain lung toxicity (Marescau et al. 1990). Artesunate also increased eicosadenoic acid, a n-6 polyunsaturated fatty acid, which can modulate inflammatory responses and be further converted to sciadonic acid, an anti-inflammatory fatty acid (Huang et al. 2011). In serum, artesunate did not cause any additional metabolic changes while dexamethasone induced alterations to 20 metabolites which were unaffected by asthma. These results indicate that corticosteroid has much broader metabolic impact than artesunate in experimental asthma, but whether they confer additional therapeutic values or impose side effect burden to patients remain to be determined.

5 Conclusions

Taken together, we revealed for the first time that artesunate possesses considerable restorative actions on airway (BALF) and systemic (serum) metabolism in experimental asthma. These effects are represented by the promotion of beneficial carbohydrates, sterols and phosphatidylcholines and the reduction of lactate and other pro-inflammatory metabolites belonging to the arginine-proline metabolic pathway. While artesunate can suppress airway inflammation and produce an array of anti-inflammatory metabolic effects similar to those by dexamethasone, it causes much less alterations in metabolites that were irrelevant to asthma. Indeed, artesunate did not affect metabolic profiles in naïve mice. These metabolomics data further strengthen the therapeutic value of artesunate for allergic asthma. Another major observation is that serum metabolite changes correlated well with airway BALF metabolite changes, implicating predictive value of serum metabolomics-derived markers for understanding asthma.

References

Barbul, A. (2008). Proline precursors to sustain mammalian collagen synthesis. *Journal of Nutrition, 138*(10), 2021S–2024S.

Cheng, C., Ho, W. E., Goh, F. Y., Guan, S. P., Kong, L. R., Lai, W. Q., et al. (2011). Anti-malarial drug artesunate attenuates experimental allergic asthma via inhibition of the phosphoinositide 3-kinase/Akt pathway. *PLoS ONE, 6*(6), e20932.

Cheng, C., Ng, D. S., Chan, T. K., Guan, S. P., Ho, W. E., Koh, A. H., et al. (2013). Anti-allergic action of anti-malarial drug artesunate in experimental mast cell-mediated anaphylactic models. *Allergy, 68*(2), 195–203.

Dai, C. L., Yao, X. L., Keeran, K. J., Zywicke, G. J., Qu, X., Yu, Z. X., et al. (2012). Apolipoprotein A-I attenuates ovalbumin-induced neutrophilic airway inflammation via a granulocyte colony-stimulating factor-dependent mechanism. *American Journal of Respiratory Cell and Molecular Biology, 47*(2), 186–195.

Fessler, M. B., Massing, M. W., Spruell, B., Jaramillo, R., Draper, D. W., Madenspacher, J. H., et al. (2009). Novel relationship of serum cholesterol with asthma and wheeze in the United States. *Journal of Allergy and Clinical Immunology, 124*(5), 967–974.

Ho, W. E., Cheng, C., Peh, H. Y., Xu, F., Tannenbaum, S. R., Ong, C. N., et al. (2012). Anti-malarial drug artesunate ameliorates oxidative lung damage in experimental allergic asthma. *Free Radical Biology & Medicine, 53*(3), 498–507.

Ho, W. E., Peh, H. Y., Chan, T. K., & Wong, W. S. F. (2014a). Artemisinins: Pharmacological actions beyond anti-malarial. *Pharmacology & Therapeutics, 142*(1), 126–139.

Ho, W. E., Xu, Y.-J., Cheng, C., Peh, H. Y., Tannenbaum, S. R., Wong, W. S. F., et al. (2014b). Metabolomics reveals inflammatory-linked pulmonary metabolic alterations in a murine model of house dust mite-induced allergic asthma. *Journal of Proteome Research*. doi:10.1021/pr5003615.

Ho, W. E., Xu, Y. J., Xu, F., Cheng, C., Peh, H. Y., Tannenbaum, S. R., et al. (2013). Metabolomics reveals altered metabolic pathways in experimental asthma. *American Journal of Respiratory Cell and Molecular Biology, 48*(2), 204–211.

Huang, Y.-S., Huang, W.-C., Li, C.-W., & Chuang, L.-T. (2011). Eicosadienoic acid differentially modulates production of pro-inflammatory modulators in murine macrophages. *Molecular and Cellular Biochemistry, 358*(1–2), 85–94.

Jiang, W., Li, B., Zheng, X., Liu, X., Cen, Y., Li, J., et al. (2011). Artesunate in combination with oxacillin protect sepsis model mice challenged with lethal live methicillin-resistant *Staphylococcus aureus* (MRSA) via its inhibition on proinflammatory cytokines release and enhancement on antibacterial activity of oxacillin. *International Immunopharmacology, 11*(8), 1065–1073.

Jin, O., Zhang, H., Gu, Z., Zhao, S., Xu, T., Zhou, K., et al. (2009). A pilot study of the therapeutic efficacy and mechanism of artesunate in the MRL/lpr murine model of systemic lupus erythematosus. *Cellular & Molecular Immunology, 6*(6), 461–467.

Jung, J., Kim, S.-H., Lee, H.-S., Choi, G. S., Jung, Y.-S., Ryu, D. H., et al. (2013). Serum metabolomics reveals pathways and biomarkers associated with asthma pathogenesis. *Clinical and Experimental Allergy, 43*(4), 425–433.

Lara, A., Khatri, S. B., Wang, Z., Comhair, S. A., Xu, W., Dweik, R. A., et al. (2008). Alterations of the arginine metabolome in asthma. *American Journal of Respiratory and Critical Care Medicine, 178*(7), 673–681.

Li, B., Li, J., Pan, X., Ding, G., Cao, H., Jiang, W., et al. (2010). Artesunate protects sepsis model mice challenged with *Staphylococcus aureus* by decreasing TNF-alpha release via inhibition TLR2 and Nod2 mRNA expressions and transcription factor NF-kappaB activation. *International Immunopharmacology, 10*(3), 344–350.

Li, Y., Wang, S., Wang, Y., Zhou, C., Chen, G., Shen, W., et al. (2013). Inhibitory effect of the antimalarial agent artesunate on collagen-induced arthritis in rats through nuclear factor kappa B and mitogen-activated protein kinase signaling pathway. *Translational Research, 161*(2), 89–98.

Marescau, B., De Deyn, P. P., Lowenthal, A., Qureshi, I. A., Antonozzi, I., Bachmann, C., et al. (1990). Guanidino compound analysis as a complementary diagnostic parameter for hyperargininemia: Follow-up of guanidino compound levels during therapy. *Pediatric Research, 27*(3), 297–303.

Mattarucchi, E., Baraldi, E., & Guillou, C. (2012). Metabolomics applied to urine samples in childhood asthma; differentiation between asthma phenotypes and identification of relevant metabolites. *Biomedical Chromatography, 26*(1), 89–94.

Mehta, A. K., Arora, N., Gaur, S. N., & Singh, B. P. (2009). Choline supplementation reduces oxidative stress in mouse model of allergic airway disease. *European Journal of Clinical Investigation, 39*(10), 934–941.

Mehta, A. K., Singh, B. P., Arora, N., & Gaur, S. N. (2010). Choline attenuates immune inflammation and suppresses oxidative stress in patients with asthma. *Immunobiology, 215*(7), 527–534.

Meurs, H., McKay, S., Maarsingh, H., Hamer, M. A. M., Macic, L., Molendijk, N., et al. (2002). Increased arginase activity underlies allergen-induced deficiency of cNOS-derived nitric oxide and airway hyperresponsiveness. *British Journal of Pharmacology, 136*(3), 391–398.

Meyts, I., Hellings, P. W., Hens, G., Vanaudenaerde, B. M., Verbinnen, B., Heremans, H., et al. (2006). IL-12 contributes to allergen-induced airway inflammation in experimental asthma. *Journal of Immunology, 177*(9), 6460–6470.

Mirshafiey, A., Saadat, F., Attar, M., Di Paola, R., Sedaghat, R., & Cuzzocrea, S. (2006). Design of a new line in treatment of experimental rheumatoid arthritis by artesunate. *Immunopharmacology and Immunotoxicology, 28*(3), 397–410.

Morris, C. A., Duparc, S., Borghini-Fuhrer, I., Jung, D., Shin, C. S., & Fleckenstein, L. (2011). Review of the clinical pharmacokinetics of artesunate and its active metabolite dihydroartemisinin following intravenous, intramuscular, oral or rectal administration. *Malaria Journal, 10*, 263.

Newton, P., Suputtamongkol, Y., Teja-Isavadharm, P., Pukrittayakamee, S., Navaratnam, V., Bates, I., et al. (2000). Antimalarial bioavailability and disposition of artesunate in acute falciparum malaria. *Antimicrobial Agents and Chemotherapy, 44*(4), 972–977.

Ng, D. P. K., Salim, A., Liu, Y., Zou, L., Xu, F. G., Huang, S., et al. (2012). A metabolomic study of low estimated GFR in non-proteinuric type 2 diabetes mellitus. *Diabetologia, 55*(2), 499–508.

Peebles, R. S., Togias, A., Bickel, C. A., Diemer, F. B., Hubbard, W. C., & Schleimer, R. P. (2000). Endogenous glucocorticoids and antigen-induced acute and late phase pulmonary responses. *Clinical and Experimental Allergy, 30*(9), 1257–1265.

Peters, M., Kauth, M., Scherner, O., Gehlhar, K., Steffen, I., Wentker, P., et al. (2010). Arabinogalactan isolated from cowshed dust extract protects mice from allergic airway inflammation and sensitization. *Journal of Allergy and Clinical Immunology, 126*(3), 648–656.

Pluskal, T., Castillo, S., Villar-Briones, A., & Oresic, M. (2010). MZmine 2: Modular framework for processing, visualizing, and analyzing mass spectrometry-based molecular profile data. *BMC Bioinformatics*. doi:10.1186/1471-2105-11-395.

Ried, J. S., Baurecht, H., Stuckler, F., Krumsiek, J., Gieger, C., Heinrich, J., et al. (2013). Integrative genetic and metabolite profiling analysis suggests altered phosphatidylcholine metabolism in asthma. *Allergy, 68*(5), 629–636.

Saude, E. J., Obiefuna, I. P., Somorjai, R. L., Ajamian, F., Skappak, C., Ahmad, T., et al. (2009). Metabolomic biomarkers in a model of asthma exacerbation: urine nuclear magnetic resonance. *American Journal of Respiratory and Critical Care Medicine, 179*(1), 25–34.

Saude, E. J., Skappak, C. D., Regush, S., Cook, K., Ben-Zvi, A., Becker, A., et al. (2011). Metabolomic profiling of asthma: diagnostic utility of urine nuclear magnetic resonance spectroscopy. *Journal of Allergy and Clinical Immunology*, *127*(3), 757–764 e, 751–756.

Sell, D. R., Strauch, C. M., Shen, W., & Monnier, V. M. (2007). 2-Aminoadipic acid is a marker of protein carbonyl oxidation in the aging human skin: Effects of diabetes, renal failure and sepsis. *Biochemical Journal, 404*, 269–277.

Serrano-Mollar, A., & Closa, D. (2005). Arachidonic acid signaling in pathogenesis of allergy: Therapeutic implications. *Current Drug Targets—Inflammation & Allergy, 4*(2), 151–155.

Smith, C. B., & Sun, Y. (1995). Influence of valine flooding on channeling of valine into tissue pools and on protein synthesis. *American Journal of Physiology, 268*(4 Pt 1), E735–E744.

Tan, S. S. L., Ong, B., Cheng, C., Ho, W. E., Tam, J. K. C., Stewart, A. G., et al. (2013). The antimalarial drug artesunate inhibits primary human cultured airway smooth muscle cell proliferation. *American Journal of Respiratory Cell and Molecular Biology, 50*(2), 451–458.

Teja-Isavadharm, P., Watt, G., Eamsila, C., Jongsakul, K., Li, Q., Keeratithakul, G., et al. (2001). Comparative pharmacokinetics and effect kinetics of orally administered artesunate in healthy volunteers and patients with uncomplicated falciparum malaria. *American Journal of Tropical Medicine and Hygiene, 65*(6), 717–721.

Weber, N., Richter, K.-D., Schulte, E., & Mukherjee, K. D. (1995). Petroselinic acid from dietary triacylglycerols reduces the concentration of arachidonic acid in tissue lipids of rats. *Journal of Nutrition, 125*(6), 1563–1568.

Weeda, E., de Kort, C. A. D., & Beenakkers, A. M. T. (1980). Oxidation of proline and pyruvate by flight muscle mitochondria of the Colorado beetle, *Leptinotarsa decemlineata* say. *Insect Biochemistry*, *10*(3), 305–311.

Wright, S. M., Hockey, P. M., Enhorning, G., Strong, P., Reid, K. B. M., Holgate, S. T., et al. (2000). Altered airway surfactant phospholipid composition and reduced lung function in asthma. *Journal of Applied Physiology, 89*(4), 1283–1292.

Xu, Y.-J., Wang, C., Ho, W. E., & Ong, C. N. (2014). Recent developments and applications of metabolomics in microbiological investigations. *TrAC Trends in Analytical Chemistry, 56*, 37–48.

Xu, X. L., Xie, Q. M., Shen, Y. H., Jiang, J. J., Chen, Y. Y., Yao, H. Y., et al. (2008). Mannose prevents lipopolysaccharide-induced acute lung injury in rats. *Inflammation Research, 57*(3), 104–110.

Xu, F. G., Zou, L., & Ong, C. N. (2009). Multiorigination of chromatographic peaks in derivatized GC/MS metabolomics: A confounder that influences metabolic pathway interpretation. *Journal of Proteome Research, 8*(12), 5657–5665.